HHS Public Access

Author manuscript

ACS Chem Neurosci. Author manuscript; available in PMC 2019 July 03.

Published in final edited form as:

ACS Chem Neurosci. 2019 March 20; 10(3): 1478–1487. doi:10.1021/acschemneuro.8b00486.

Cholesterol Functionalization of Gold Nanoparticles Enhances Photoactivation of Neural Activity

Joao L. Carvalho-de-Souza[†], **Okhil K. Nag**[‡], **Eunkeu Oh**[§,‖], **Alan L. Huston**[§], **Igor Vurgaftman**[§], **David R. Pepperberg**[⊥], **Francisco Bezanilla**[†], and **James B. Delehanty**[*,‡]

[†]Department of Biochemistry and Molecular Biology and Institute for Biophysical Dynamics, The University of Chicago, Chicago, Illinois 60637, United States

[‡]Center for Bio/Molecular Science and Engineering, Naval Research Laboratory, Code 6900, 4555 Overlook Avenue SW, Washington, DC 20375, United States

[§]Optical Sciences Division, Naval Research Laboratory, Code 5600, 4555 Overlook Avenue SW, Washington, DC 20375, United States

[‖]Key W Corporation, Hanover, Maryland 21076, United States

[⊥]Lions of Illinois Eye Research Institute, Department of Ophthalmology and Visual Sciences, University of Illinois at Chicago, Chicago, Illinois 60612, United States

Abstract

Gold nanoparticles (AuNPs) attached to the extracellular leaflet of the plasma membrane of neurons can enable the generation of action potentials (APs) in response to brief pulses of light. Recently described techniques to stably bind AuNP bioconjugates directly to membrane proteins (ion channels) in neurons enable robust AP generation mediated by the photoexcited conjugate. However, a strategy that binds the AuNP to the plasma membrane in a non protein-specific manner could represent a simple, single-step means of establishing lightresponsiveness in multiple types of excitable neurons contained in the same tissue. On the basis of the ability of cholesterol to insert into the plasma membrane, here we test whether AuNP functionalization with linear dihydrolipoic acid-poly(ethylene) glycol (DHLA-PEG) chains that are distally terminated with cholesterol (AuNP–PEG–Chol) can enable light-induced AP generation in neurons. Dorsal root ganglion

[*]Corresponding Author james.delehanty@nrl.navy.mil.

Author Contributions

J.L.C. performed the DRG photoactivation experiments. O.K.N. made the AuNP–PEG–Chol conjugates and performed cell labeling and toxicity tests. E.O. synthesized and characterized the AuNPs and, along with A.L.H. and I.V., calculated the theoretical AuNP photothermal responses. J.L.C., D.R.P, F.B., and J.B.D. jointly conceived of the AuNP bioconjugation and plasma membrane tethering concept. All authors contributed to the preparation of the manuscript.

DEDICATION

We dedicate this manuscript to the memory of coauthor David R. Pepperberg who helped conceive of the cholesterol functionalization strategy.

ASSOCIATED CONTENT

Supporting Information

The Supporting Information is available free of charge on the ACS Publications website at DOI: 10.1021/acschemneuro.8b00486. TEM and spectral analysis of AuNPs and AuNP conjugates, analysis of plasma membrane labeling with AuNP–PEG–Chol, and theoretical analysis of predicted AuNP temperature changes (PDF)

Notes

The authors declare no competing financial interest.

(DRG) neurons of rat were labeled with 20 nm diameter spherical AuNP–PEG–Chol conjugates wherein ~30% of the surface ligands (DHLA-PEG-COOH) were conjugated to PEG–Chol. Voltage recordings under current-clamp conditions showed that DRG neurons labeled in this manner exhibited a capacity for AP generation in response to microsecond and millisecond pulses of 532 nm light, a property attributable to the close tethering of AuNP–PEG–Chol conjugates to the plasma membrane facilitated by the cholesterol moiety. Light-induced AP and subthreshold depolarizing responses of the DRG neurons were similar to those previously described for AuNP conjugates targeted to channel proteins using large, multicomponent immunoconjugates. This likely reflected the AuNP–PEG–Chol's ability, upon plasmonic light absorption and resultant slight and rapid heating of the plasma membrane, to induce a concomitant transmembrane depolarizing capacitive current. Notably, AuNP–PEG–Chol delivered to DRG neurons by inclusion in the buffer contained in the recording pipet/electrode enabled similar light-responsiveness, consistent with the activity of AuNP–PEG–Chol bound to the inner (cytofacial) leaflet of the plasma membrane. Our results demonstrate the ability of AuNP–PEG–Chol conjugates to confer timely stable and direct responsiveness to light in neurons. Further, this strategy represents a general approach for establishing excitable cell photosensitivity that could be of substantial advantage for exploring a given tissue's suitability for AuNP-mediated photocontrol of neural activity.

Graphical abstract

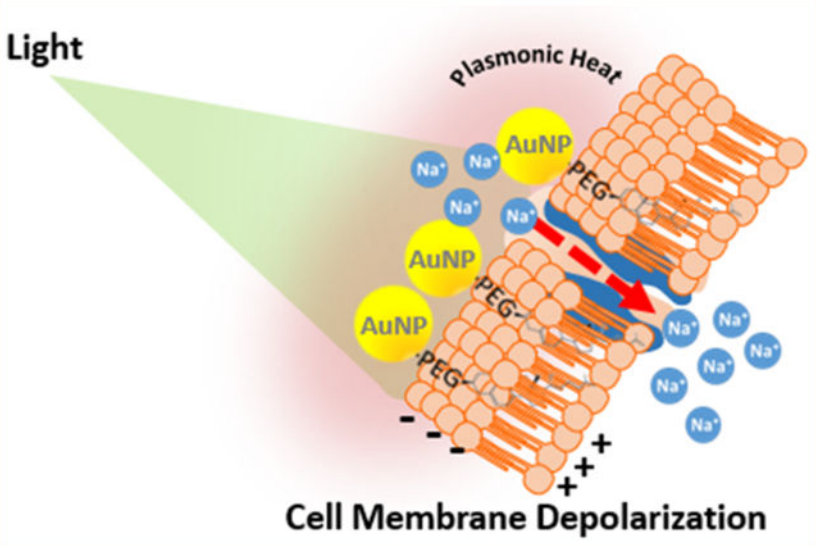

Keywords

Gold nanoparticles; cholesterol; nanoparticle functionalization; photosensitivity; neural photoactivation; action potential; optocapacitance; dorsal root ganglion cell

INTRODUCTION

The interfacing of photophysically active nanomaterials with biological tissue is a rapidly growing area of research in fundamental and clinically relevant biomedicine. Gold nano-

particles (AuNPs), in particular, possess unique electronic and plasmonic properties that make them valuable tools for plasmonic heating and radiosensitization in current cancer therapy investigations.[1–3] In addition, recent studies with neurons have demonstrated a markedly different application of AuNP-mediated plasmonic heating: action potential (AP)-firing. In the work presented here, AuNPs were interfaced with the neuronal plasma membrane using a cholesterol moiety appended to the AuNP surface. A rapid and small (non-damaging) increase in membrane temperature, induced by AuNP photoexcitation, facilitated the controlled generation of APs by the neuron.

The immediate foundation and motivation for the present study comes from recent investigations by Carvalho-de-Souza et al. of AP generation in neurons using photoexcited AuNPs.[4,5] That work was inspired by Shapiro et al., who showed temperature-dependent changes in membrane capacitance are the basis of the infrared light's effect on excitable tissues.[6] Using dorsal root ganglion (DRG) neurons, an extensively studied type of excitable cell, Carvalho-de-Souza et al. showed that brief (millisecond) light pulses photoexcite membrane-tethered AuNPs and induce APs. Results obtained in these studies indicated that a modest local heating of the membrane (as small as 1–2 °C as determined in AuNP-tethered lipid bilayers) due to the dissipation of plasmonically absorbed light energy produces a highly transient, depolarizing capacitive current that opens nearby voltage-gated sodium channels (Na_Vs).[4] The Carvalho-de-Souza et al. studies employed 20 nm spherical AuNPs that were bound to the DRG neuron plasma membrane. For example, one of the membrane-tethering strategies used was AuNP–streptavidin conjugates assembled with biotinylated Ts1 neurotoxin, a peptide that binds directly to Na_Vs without blocking them. Recent work by Kubota et al. successfully employed an inactive version of Ts1 (Ts1 S14R) to functionalize AuNPs.[7] Additional strategies involved the use of a primary antibody directed against the native ion channels TRPV1 or P2X3. In this antibody-based approach, the AuNPs were functionalized with a secondary antibody against the anti-TRPV1 or anti-P2X3 primary antibody. Following pretreatment of the cells with the appropriate primary antibody, secondary antibody–AuNP conjugates bound specifically to the primary antibody-decorated membrane proteins. While effective, this multistep labeling process resulted in large immunocomplexes that positioned the AuNP tens of nanometers from the exofacial leaflet of the membrane. DRG neuron responsiveness to light could also be established by incubation of the cells with nonfunctionalized (i.e., unconjugated) AuNPs that were allowed to settle onto the plasma membrane.[4] However, in contrast to the photoactivation mediated by conjugates specifically targeted to Na_Vs, TRPV1, or P2X3, photosensitization by nonfunctionalized AuNPs was quickly eliminated by washing/perfusion that removed these un-attached AuNPs from the cell periphery.

The present study addresses a fundamental question raised by the above-summarized and other findings reported by Carvalho-de-Souza et al. That is, both experimental data and modeling indicate that AuNP-mediated photogeneration of APs requires rapid and efficient transfer of the AuNP's dissipated heat energy to the plasma membrane while minimizing energy loss to the surrounding aqueous medium.[4,5] Thus, close tethering of the AuNP to the membrane bilayer is necessary for efficient heat transfer. While this can be achieved by binding of the AuNP to native membrane ion channels, it remains unclear if attachment to intrinsic membrane proteins is necessary for suitable heat transfer to the plasma membrane

or, alternatively, whether a more general methodology for interfacing the AuNP with the membrane could enable efficient AuNP-facilitated photogeneration of APs.

To that end, in the present study, we sought to develop a general bioconjugation strategy that would allow for the facile tethering of AuNPs to the plasma membrane of electrically excitable cells. Specifically, our hypothesis was that the functionalization of AuNPs with a pan-specific membrane-interfacing moiety could realize AuNP bioconjugates for probing the responsivity of multiple, disparate types of excitable neurons in a given tissue without the need to target the AuNPs to specific membrane proteins. On the basis of abundant literature evidence for the affinity of cholesterol for biological membranes[8,9] and its ability to append a variety of AuNPs to the plasma membrane,[10–12] we hypothesized that a AuNP conjugate displaying cholesterol on its surface could serve as a robust and generalized means of tethering the AuNP to the plasma membrane. We further hypothesized that joining of the hydrophobic cholesterols to the AuNP through linear poly(ethylene glycol) (PEG) chains would facilitate conformational flexibility for proximal tethering to the membrane while providing the requisite colloidal stability for efficient cellular labeling. For this study, we specifically chose 20 nm diameter AuNPs as our photoactivatable material given their significant plasmonic absorption, amenability to bioconjugation, and well-established biocompatibility.[13–15] While other materials including mesostructured silicon,[16] photosensitive proteins[17] and polymers,[18] carbon-based,[19] and semiconductor materials[20] are available, they can pose significant challenges such as interfacing them controllably with the 5 nm expanse of the plasma membrane, culturing the cells on engineered surfaces, or the need for genetic manipulation of the targeted cells. Further, the 20 nm diameter AuNPs used herein offer the optimal balance between maximal plasmonic absorption and minimal incident photon loss due to scattering that is characteristic of larger AuNPs.[21]

We show here that AuNPs, when appended with PEGylated cholesterol (AuNP–PEG–Chol), display robust plasma membrane labeling of HEK 293T/17 cells upon incubation at very low AuNP concentrations (1–3 nM). In DRG neurons isolated from rat, labeling of the plasma membrane with 1 nM AuNP–PEG–Chol is sufficient to enable AuNP-mediated firing of APs. We further confirm that AuNP-mediated depolarization of the DRG neuron is dependent not only on the presence of PEG–Chol on the AuNP surface, but that the magnitude of the subthreshold depolarization response and attainment of AP generation threshold track positively with the duration of the light pulse across a range of stimulating laser powers. We also present evidence that the intracellular delivery of AuNP–PEG–Chol by its inclusion in the buffer contained within the patch pipet used for electrophysiological recording can confer photosensitivity upon the cell. Furthermore, analysis of the relationship between laser pulse duration and pulse energy at AP generation threshold shows excellent agreement with the predicted power law relationship governing the generation of light-induced capacitive currents in the plasma membrane.[5] The findings reported here provide a generalized strategy for the production of photoactive AuNP bioconjugates for robust light-stimulated AP generation in neurons that is not dependent on targeting of the AuNP to specific membrane-resident proteins.

RESULTS

To undertake our study of AuNP-mediated photoactivation, we synthesized 20 nm AuNPs capped with thioctic acid ligands grafted to PEG chains (MW 600) that terminated in carboxyl groups (Figure 1A). The rationale for this material selection was that the 20 nm AuNP (size confirmed by transmission electron microscopy (Supporting Information (SI) Figure S1)) possesses a large surface plasmon band peak at ~520 nm that is efficiently excited with a 532 nm laser line, and it has a minimal scattering cross section (less than 1% of total extinction) compared to larger diameter AuNPs or Au nanorods.[22]

Successful conjugation was confirmed by agarose gel electrophoresis, where it was clear that decoration of the AuNP surface with the PEG–Chol and/or PEG–FITC moieties significantly reduced the migration of the AuNPs toward the cathode (SI Figure S2A). Importantly, the conjugation did not abrogate the characteristic absorption of the AuNP, nor did the AuNP significantly quench the luminescence of the fluorescein (SI Figure S2B). Dynamic light scattering analysis also confirmed successful conjugation, as the hydrodynamic diameter of the AuNP–PEG–Chol and -PEG–Chol/PEG–FITC conjugates increased to ~30 and ~35 nm, respectively, from ~20 nm (SI Figure S2C). Zeta-potential measurements showed a significant decrease in the negative surface charge upon conjugation of AuNP with PEG–Chol and/or PEG–FITC (SI Figure S2D). Cumulatively, these data provided strong evidence of the successful conjugation of PEG–Chol and/or PEG–FITC to the surface of the AuNP. Overall, the conjugation procedure resulted in AuNPs that maintained sufficient negative surface charge (–15 to –20 mV) to ensure colloidal stability in solution.

We next assessed the cellular labeling efficiency of the conjugates. HEK 293T/17 cells were labeled with varying concentrations of the AuNP–PEG–Chol/PEG–FITC conjugates, and it was determined that 3 nM was adequate to achieve robust labeling of the plasma membrane after only a short (20 min) incubation period (SI Figure S3). Notably, minimal internalization of the conjugates was observed, even 2 h after initial labeling and washing (data not shown), and we observed negligible binding of AuNPs lacking the Chol moiety to HEK 293T/17 cell monolayers (SI Figure S3), consistent with our previous work on other PEG–Chol conjugated NP systems.[11] It is worth noting that the AuNP concentrations used here for membrane labeling photoactivation (*vide infra*) are two orders of magnitude lower than those we have used previously for studies of cellular AuNP uptake/internalization driven by cell-penetrating peptides.[23] These data clearly demonstrate the nature of the PEG–Chol ligand system as a facile yet robust means by which to append AuNPs to the plasma membrane with persistent membrane residence that is not attainable using peptides or proteins that often drive endocytosis and cellular internalization of the AuNP conjugates.[23]

AuNP-Mediated Photoactivation of Action Potentials.

Having demonstrated the efficient tethering of AuNP–PEG–Chol/PEG–FITC bioconjugates to the plasma membrane, we next sought to determine the ability of AuNP–PEG–Chol to photoactivate APs in neurons upon short laser pulse illumination. The photoactivation experiments were conducted on single current-clamped DRG neurons isolated from newborn rats. The cells were prepared and mounted in an optical system coupled with a current-clamp

membrane voltage recording system according to the procedure described previously.[4,5] The experiments were performed at an ambient room temperature of ~20 °C. For plasma membrane labeling, DRG cells (a coculture of neurons and non-neuronal cells) were incubated overnight at 37 °C in growth medium containing AuNP–PEG–Chol at a concentration of 1 nM (see methods). Next, unbound AuNP–PEG–Chol in the medium were removed by washing the dish with plain Tyrode's solution, and the dish was then transferred to the recording apparatus for electrophysiological study.

Figure 2 shows representative photoactivated responses obtained for light-induced subthreshold depolarizations in DRG neurons that were labeled with 1 nM AuNP–PEG–Chol conjugates. Cells incubated overnight with 1 nM AuNP-PEG-COOH (no Chol) or cells incubated with medium alone were included as controls. Here and in the experiments described below, the investigation of each cell involved an initial test of photosensitivity at several locations along the cell body. This was achieved by shifting the position of the laser to direct the stimulating beam onto different regions of the plasma membrane. Each stimulated area was ~5 μm in diameter (see Experimental Methods). Observed photoresponsiveness at these different locations ranged from an AP generation response to a negligible response that was similar to that exhibited by AuNP-untreated cells. We attributed this to the slight heterogeneity of plasma membrane labeling with the AuNP–PEG–Chol bioconjugates (i.e., certain regions of the plasma membrane were rich in AuNPs while other regions had little to no labeling). This is consistent with the preferential affinity of the Chol-decorated AuNPs for lipid raft micro-domains in the plasma membrane as we have observed in our previous studies.[10,11] Upon identification of the maximally photoresponsive region of the plasma membrane, no further movement of the laser beam was made, and this maximally sensitive region was used for detailed characterization of the AuNP–PEG–Chol-induced photoresponsiveness on the cells. As shown in Figure 2A, the peak amplitude of the response induced by a 0.5 ms light pulse (112 μJ) in cells labeled with AuNP–PEG–Chol greatly exceeded (by ~10 mV) the response induced in AuNP-PEG-COOH-labeled cells exposed to a higher energy (225 μJ) flash of 1 ms duration as well as cells not treated with AuNPs. Figure 2B illustrates the dependence of the subthreshold responses of AuNP–PEG–Chol-treated and control cells as a function of the duration of a light pulse of fixed power (225 mW). Cumulatively, these data demonstrate the ability of the photoexcited AuNP–PEG–Chol conjugates to specifically induce robust depolarization over a considerable range of flash durations across the μs to msec time regime.

Action potentials induced in AuNP–PEG–Chol-treated DRG neurons by brief light pulses exhibited waveform kinetics similar to those exhibited by previously studied AuNP preparations.[4,5] Figures 3A–C show representative action potentials obtained from three separate AuNP–PEG–Chol-labeled neurons as a function of the laser power and duration and thus, energy (SI Figure S4). For each cell, increasing the pulse duration produced subthreshold depolarizing responses of progressively increasing peak amplitude until the threshold for action potential depolarization of the cell was reached. Figure 3D, which shows DRG neuron responses to stimuli of fixed duration obtained from one of the cells in panel C, illustrates the marked changes in peak amplitude and kinetics of the response produced by increasing the energy of the AuNP-exciting light pulse.

As noted in the Introduction, previous reports indicated the role of an induced depolarizing capacitive current as the mechanism by which heating of the membrane by plasmonically photoexcited AuNPs induces AP generation.[4–6] This depolarizing capacitive current is reflected as a graded passive depolarization of the plasma membrane resting potential, i.e., distinct from the active depolarizing ionic current associated with Na_V activation/opening that undergoes a positive feedback and underlies the rising phase of the AP itself. The temperature increase for the experiments conducted herein can be estimated using the solution of the steady state heat-conduction equation for a spherical AuNP heat source, assuming that the thermal conductivity of the AuNP is much higher than that of its surroundings.[24,25] The resulting expression is

$$\Delta T(r) = \frac{IQ_{\text{abs}}R}{4k_{\text{m}}} r \leq R$$

$$\Delta T(r) = \frac{IQ_{\text{abs}}R}{4k_{\text{m}}} \frac{R}{r} r > R$$

where R is the AuNP radius (10 nm), r is the distance from the center of the AuNP, I is the intensity of the incident pump in W/cm^2, Q_{abs} is the relative absorption cross section normalized to the cross section of the AuNP (0.47) (i.e. $\sigma_{\text{abs}} = Q_{\text{abs}}\pi R^2$), and k_{m} is the thermal conductivity of the surrounding medium. The calculated absorption cross section of the 20 nm AuNP used here was $\sigma_{\text{abs}} = 1.5 \times 10^{-12}$ cm^2 based on absorption measurements.[13] For a AuNP interfaced with the membrane and surrounded mostly by water, this leads to an estimated $\Delta T = 11$ °C immediately at the AuNP surface under the pumping conditions of the experiments described herein. Using this relation, the estimated temperature increase of the surrounding medium was plotted as a function of distance from the surface of the AuNP (SI Figure S5). The experimental conditions used here were: average laser power =114 mW, focused spot size ~5 μm, and exposure time = 0.5 ms. Considering the solution persistence length of the PEG ligand and the hydrodynamic size of AuNP–PEG–Chol (~32 nm), the maximum temperature increase just at the surface of the cell's plasma membrane (~6 nm from the surface of the AuNP) was estimated to be ~7 °C. This value agrees well with that determined by Govorov et al. based on AuNP size and light flux.[26]

Given the apparent dependence of the passive graded depolarization on the rate of membrane temperature increase and the onset of depolarization primarily within microseconds of pulse delivery,[5] we hypothesized that with a laser pulse power that produces a membrane depolarization that does not excessively exceed the AP generation threshold, the magnitude of passive depolarization in AuNP–PEG–Chol-treated DRG neurons would be near constant under conditions in which the pulse duration is within the microsecond to millisecond range. To test this hypothesis, we performed repetitive laser stimulation (100 pulses every 3 s for 300 s time window) on multiple AuNP–PEG–Chol-labeled DRG neurons with laser pulses of differing duration and power that induced AP generation in ~70% of trials. As shown in Figure 4A, the resting potential exhibited by these

cells immediately prior to each laser stimulation was remarkably constant (–66.8 ± 0.1 mV) over the 5 min experimental window.

The green symbols in Figure 4A indicate the peak value of membrane potential associated with passive depolarization upon laser pulses that varied from 100 μs to 1.8 ms in duration. Again, the average value of this peak potential was remarkably constant over the period of investigation (–48 ± 0.1 mV). These data are represented graphically in Figure 4B. The data shown in Figure 5 show the variation in flash energy (E_{Th}) (in nJ) as a function of pulse duration (in μs) obtained from a total of six AuNP–PEG–Chol-labeled DRG neurons. It is described by the equation:

$$E_{\mathrm{Th}} = a \times D^{b}$$

where E_{Th} is the flash energy necessary to depolarize the plasma membrane to its threshold for AP firing, a is an independent term that relates to the number of AuNPs and their average distance to the membrane, D is the duration of the laser pulse, and b is the power law that governs the relationship. The dashed line in Figure 5 shows the fit of the power law function to these data.[5] Interestingly, these results show that the value of the exponent b (0.75) of the fitted function was essentially the same as those determined for the previously studied particles,[4,5] consistent with the concept that the AuNP–PEG–Chol's photosensitizing action involves AuNP-dependent membrane heating coupled with the production of a transmembrane capacitive current. Importantly, cytotoxicity analysis of the AuNP labeling procedure (in HEK 293T/17 cells) and accompanying photoactivation procedure (in DRG neurons) showed negligible effects on cellular proliferation and viability, respectively (Figure S6).

Heretofore, all of the experiments were performed on DRG neurons that were labeled with AuNP–PEG–Chol conjugates by incubating the cells with the conjugate materials in culture media, followed by the removal of unbound conjugates by washing. Thus, the AuNPs were tethered to the exofacial (outer) leaflet of the plasma membrane. However, we were further interested in asking whether AuNP–PEG–Chol conjugates delivered to and tethered to the cytofacial (inner) leaflet of the plasma membrane could render the DRG neurons equally photoresponsive compared to when they are present on the exofacial leaflet of the bilayer. To address this, the AuNP–PEG–Chol conjugates were included in the buffer contained in the patch pipet used for current-clamp recording (Figure 6). In this approach, the standard pipet solution (see Experimental Methods) was supplemented with AuNP–PEG–Chol at a concentration of 1.5 nM, and the period between immersion of the pipet into the cell-bathing solution and pipet contact with the cell under study was minimized (less than 3 min) to minimize dilution of the pipet solution into the bathing medium. On the basis of our prior work with NP–cholesterol bioconjugates,[10] the delivery of the AuNPs to the cellular cytosol presumably results in the attachment of the AuNPs to the inner leaflet of the plasma membrane. Once the target cell was successfully patched, the laser beam was iteratively moved to illuminate differing regions of the cell with 45 mW laser pulses of varying duration. As illustrated in (Figure 6A), each of the APs displayed amplitudes similar to those observed in previous experiments in which delivery of the AuNP–PEG–Chol was from the

extracellular medium (Figures 2–5). We did observe, however, that the delay preceding action potential initiation showed considerable variation (ranging from 20 to 50 ms). These differing delays in AP firing may be attributable in part to fluctuations in the resting potential that could lead to shifts in the AP voltage threshold. These assumptions are more reasonable when one considers AuNPs are present inside the patch pipet, consequently potentially interfering with the seal between the membrane and the pipet. Notably, however, the relationship between pulse duration and threshold energy (E_{Th}) for action potential generation in this "intracellular" AuNP delivery method was well-described by the same power law function used to analyze the "extracellular" AuNP delivery experiments (exponent $b = 0.62$), demonstrating a strong correlation in the power law governing action potential generation between the two AuNP delivery methodologies.

DISCUSSION

The results presented herein show that AuNPs functionalized with PEGylated cholesterol and delivered to DRG neurons *in vitro* establish the capacity for efficient light-induced action potential generation. As described above, these experiments build on those of recent studies that demonstrated DRG neuron photoresponsiveness enabled by AuNPs that were tethered directly to voltage-gated sodium channels. Here we asked whether cholesterol, an integral component of the mammalian cell plasma membrane that has been demonstrated to effectively append myriad AuNPs to the cell surface,[10,11,27,28] can function as a pan-specific plasma membrane-tethering ligand of AuNPs to afford a similar establishment of cell photoresponsiveness. In the current study, we synthesized 20 nm diameter AuNPs that were covalently capped with a discrete amount of PEG_{2000}–Chol ligands. Our findings, indeed, provide strong evidence that these materials, when delivered to cells at low nM concentrations, efficiently mediate photoinduced action potentials in DRG neurons. Given the fact that cholesterol is ubiquitously present in the membranes of a wide range of electrically excitable cells (including both neurons and muscle cells), this cholesterol-based tethering approach avails what we believe is an important new avenue for application of the AuNP technique. That is, the labeling of cells with AuNP–PEG–Chol conjugates could serve as a valuable approach by which to interrogate a new cell type or tissue for the ability of one or more of the constituent cell types to be capable of AuNP-enabled photoresponsiveness.

The AuNP–PEG–Chol conjugates' photosensitizing action provides support for an optocapacitive basis of this activity. On the basis of earlier findings, a key feature of the optocapacitance mechanism is the requirement for the AuNP-based conjugate to rapidly and efficiently dissipate the energy of an absorbed laser pulse to the plasma membrane.[4,5] This process depends critically, in turn, on the close proximity of the AuNP to the membrane. In this context, the PEG–Chol anchor of the AuNP described herein offers the distinct advantage of positioning the AuNP extremely close to the membrane surface. The PEG_{2000} component of the AuNP capping ligand has a predicted hydrated persistence length of ~10 nm.[29] This distance is considerably less than the several tens of nanometers distance anticipated in the case where the AuNP is anchored to plasma membrane protein channels through a primary–secondary antibody ensemble or biotin–streptavidin assembly.[4] Clearly, this feature of the AuNP–PEG–Chol conjugate system studied here underlies the observed robust photoresponsiveness enabled by this conjugate.

Another noteworthy finding of this study is that the ability of the AuNP–PEG–Chol conjugates to mediate photoresponsiveness when appended to the cytofacial side of the plasma membrane. Indeed, inclusion of AuNP–PEG–Chol within the fluid contained in the recording pipet established photoresponsiveness generally similar to that enabled by overnight incubation of the cells with AuNP–PEG–Chol-containing extracellular medium. This mode of photoexcitability may have important applications in neuroscience by targeting specific neurons via axonal transport of known pathways. Given that membrane-tethering by cholesterol can in principle be mediated at the intracellular as well as the extracellular face of the plasma membrane, the present findings strongly suggest that both sides of the plasma membrane can bind AuNP–PEG–Chol and undergo optocapacitive depolarization induced by the bound conjugate. While it is likely that a certain percentage of the membrane-appended conjugates are internalized via endocytosis or regular membrane recycling, our data clearly demonstrate that the Chol-mediated membrane tethering approach avails labeling of the plasma membrane that facilitates DRG neuron photoresponsiveness over the experimental window shown here.

The present results provide proof-of-principle for excitable cell photosensitization by AuNPs functionalized with the general membrane-anchoring moiety, cholesterol. With respect to the waveform kinetics of generated APs induced by AuNP–PEG–Chol treatment and the likely optocapacitive basis of this action, AuNP–PEG–Chol-mediated photoresponsiveness is remarkably similar to that mediated by AuNP conjugates that target specific plasma membrane proteins[4] as well as unconjugated AuNPs that interface with the plasma membrane upon gravitational settling.[5] One key difference noted between the Chol-tethered AuNPs used in the present study and AuNPs specifically bound to Na_Vs using antibodies or unconjugated AuNPs (in previous works) is that the value of the linear coefficient obtained for AuNP–PEG–Chol-treated cells (delivered both extracellularly and intracellularly) is considerably higher. In the case of cells labeled with AuNP–PEG–Chol conjugates, it is likely that the lower density of AuNPs per unit area of the membrane plays a role in this functional observation. Coupled with this is the fact that the PEG–Chol moiety (and other lipophilic surface ligands) are known to promote “clustering” of attached AuNP cargos into concentrated lipid raft domains, which can promote local, regiospecific microenvironments of concentrated AuNPs on the membrane.[30–32] Indeed, the need for considerably lower concentrations of AuNPs in the present study (1 nM) compared to previous studies of AuNP cellular labeling/ delivery using peptides[14,23] suggests that this attribute can be exploited for the codelivery of AuNP-appended drugs or other therapeutics. Studies are currently underway in our laboratory to discern the “tunability” of the AuNP–PEG–Chol system by controlling the AuNP-membrane separation distance using PEG chains of varying lengths. Additionally, future studies will focus on the implementation of the present AuNP–PEG–Chol AuNPs for the simultaneous photoinduced AP generation and release of delivery of light-cleavable drug cargos.

EXPERIMENTAL METHODS

Materials.

All chemicals were purchased from Sigma (St. Louis, MO) and used as received unless otherwise mentioned. Dulbecco's phosphate buffered saline (DPBS), 4-(2-hydroxyethyl)-1-piperazinee-thanesulfonic acid (HEPES, 1M), Dulbecco's modified Eagle's medium (DMEM) containing 25 mM HEPES (DMEM-HEPES), 1-ethyl-3-(3-(dimethylamino)propyl)carbodiimide (EDC), and *N*-hydroxysulfosuccinimide sodium salt (NHSS) were obtained from Life Technologies (Grand Island, NY). Cholesterol poly(ethylene glycol) amine hydrochloride (Chol–PEG–NH_2HO, MW 2000) was purchased from Nanocs Inc. (NY, United States). Trypsin (Cat # TRL3) and fetal bovine serum (FBS, Cat. # 30–2020) were purchased from Worthington Biochemical Corp. (Lakewood, New Jersey, United States) and ATCC (Manassas, Virginia, United States), respectively. Earle's balanced salt solution (EBSS) was prepared by adjusting a solution containing 132 mM NaCl, 5.3 mM KCl, 1 mM NaH_2PO_4, 10 mM HEPES, and 5.5 mM glucose to pH 7.4. Tyrode's solution (also the extracellular solution) was prepared by adjusting a solution containing 132 mM NaCl, 4 mM KCl, 1.8 mM $CaCl_2$, 1.2 mM $MgCl_2$, 10 mM HEPES, and 5 mM glucose to pH 7.4. Patch pipet solution was prepared by adjusting a solution containing 150 mM KF, 10 mM NaCl, 4.5 mM $MgCl_2$, 2 mM ATP, 9 mM EGTA, and 10 mM HEPES to pH 7.4.

Synthesis of AuNPs.

AuNPs were synthesized directly in aqueous phase by using a seed growth method in the presence of citric acid and ascorbic acid. For 10 nm seed AuNPs, 200 μL (2.0×10^{-5} mol) of 100 mM tetrachloroauric (III) acid ($HAuCl_4 \cdot 3H_2O$) aqueous stock solution and 200 μL (2.0×10^{-5} mol) of 100 mM of citric acid aqueous solution were added to the 50 mL of deionized water, and the reaction mixture was vigorously stirred at room temperature for 5 min. Then, 200 μL (4.0×10^{-5} mol) of 200 mM L-ascorbic acid aqueous solution was added to the reaction mixture, followed by vigorous stirring for next 30 min. Next, the growth solution was prepared with 0.4 mM $HAuCl_4$ and 0.8 mM sodium citrate in 50 mL of deionized water. To synthesize 20 nm AuNPs, 7 mL of seed AuNP solution was added to the growth solution followed by addition of L-ascorbic acid (2 mM final concentration). The reaction mixture was stirred for 3 h at room temperature and kept without stirring for additional 24 h to complete the AuNP synthesis reaction and deactivate the ascorbic acid. The reaction of AuNPs was confirmed by the red shift of the surface plasmon band peak and the decrease of the ascorbic acid and aurate peaks in the near UV region (<300 nm) using UV–vis spectroscopy. The final AuNP sizes were confirmed by TEM and DLS measurements.

Ligand Exchange of AuNPs.

For the ligand exchange reaction, the presynthesized AuNPs were added to a molar excess of TA–PEG–COOH (MW of PEG ~600) as described previously.[14] Briefly, 10 mL of as-synthesized citrate-modified AuNPs were mixed with 25 μL of 100 mM stock TA–PEG–COOH aqueous stock solution. The solution was stirred for 8 h, and the AuNP dispersion was purified from free ligands by three cycles of centrifugation using a centrifugal

membrane filtration device (10–30 kDa molecular weight cutoff, Millipore Corporation, Billerica, MA) and deionized water. AuNP concentration was determined as described previously using the known extinction coefficient (molar absorption) of 20 nm spherical AuNPs (~9.2×10^8 M^{-1} cm^{-1} at 520 nm).[13]

UV–Vis Spectroscopy.

Electronic absorption spectra were recorded using a Shimadzu UV-1800 UV–vis spectrophotometer to monitor the changes of spectra before and after biomolecule conjugation on Au-PEG.

Transmission Electron Microscopy and Energy-Dispersive X-ray Spectroscopy.

Structural characterization and elemental analysis of AuNPs were carried out using a JEOL 2200-FX analytical high-resolution transmission electron microscope with a 200 kV accelerating voltage. Samples for TEM were prepared by spreading a drop (5–10 μL at 10 nM) of the filtered AuNPs dispersion (filtered by using 0.25 μm syringe filters (Millipore)) onto an ultrathin carbon/holey support film on a 300 mesh Au grid (Tedpella, Inc.) and allowing it to dry. Individual particle sizes were measured using a Gatan Digital Micrograph (Pleasanton, CA). Average sizes along with standard deviations were extracted from analysis of at least 50–100 AuNPs.

Dynamic Light Scattering.

DLS measurements were carried out using ZetaSizer NanoSeries equipped with a HeNe laser source (λ = 633 nm) (Malvern Instruments Ltd., Worcestershire, UK) and analyzed using Dispersion Technology Software (DTS, Malvern Instruments Ltd., Worcestershire, UK). Similar concentration of TEM samples were loaded into disposable cells, and data were collected at room temperature. All the samples were prepared in 0.1× PBS buffer (pH 7.4). For each sample, the autocorrelation function was the average of 5 runs of 10 s each (repeated about 3–6 times). CONTIN analysis was then used to determine the AuNP number versus hydrodynamic size for the dispersions studied.

Preparation of AuNP Conjugates.

AuNPs capped with TA–PEG–COOH were covalently conjugated to NH_2–PEG_{2000}–Chol and NH_2–PEG_{2000}–FITC via carbodiimide chemistry. A stock solution (if NH_2–PEG_{2000}–Chol (10 mM) or NH_2–PEG_{2000}–FITC (10 mM) was prepared in water. A stock solution containing NHSS (25 mM) or EDC (500 mM) was prepared in PBS (10×, pH 7.0) buffer. An aliquot (10 μL) of the freshly prepared stock solution of NHSS and EDC was immediately added to 1.0 mL of 34 nM AuNP–TA–PEG–COOH in PBS (10×, pH 7.0) buffer and stirred for 5 min. For conjugation of NH_2–PEG_{2000}–Chol, an aliquot (10 μL) of stock solution of NH_2–PEG_{2000}–Chol was added to this mixture and stirred for 2 h. For conjugation of NH_2–PEG_{2000}–Chol and NH_2–PEG_{2000}–FITC to same AuNP–TA–PEG–COOH, aliquots of stock solutions of NH_2–PEG_{2000}–Chol (7.0 μL) and NH_2–PEG_{2000}–FITC (3.0 μL) were added to this mixture and stirred for 2 h. The reaction mixture was briefly centrifuged, and the supernatant was subjected to size exclusion chromatography using a PD-10 column equilibrated with DPBS (0.1×). The AuNP band was collected and analyzed by agarose

(1%) gel electrophoresis. The as-synthesized AuNP conjugates (AuNP–TA–PEG–PEG–Chol and AuNP–TA–PEG–PEG–Chol/FITC) were characterized for their particle concentration, size, and charge. Particle size distribution zeta-potential were measured as described above. While the absolute composition of the functionalized NPs were not determined, the laser activation of cells and fluorescence labeling data strongly support that the intended functional groups were present on the AuNPs.

HEK 293T/17 Cell Culture, Cellular Staining, and Imaging for AuNP–PEG–Chol/FITC.

HEK 293T/17 cells (ATCC # CRL-11268, Manassas, VA) were cultured at 37 °C in a humidified atmosphere containing 95% air/5% CO_2. Cells were cultured in complete growth medium defined as follows: DMEM (purchased from ATCC) supplemented with 10% (v/v) heat-inactivated fetal bovine serum (ATCC) and 1% antibiotic/antimycotic (Sigma). Cells were cultured in T25 flasks, and a subculture was performed every 3–4 days. Cellular AuNP delivery experiments were performed using cells between passages 5 and 15, and the efficiency of membrane labeling was consistent across this passage number range. Cells were seeded to 35 mm Petri dish with 14 mm glass bottom insert (#1.0 cover glass, MatTek Corp., MA, United States) at a density of ~7×10^4 cells/mL (3 mL/well). Dishes were coated with fibronectin (20 μg/mL) in DPBS before adding the cell suspension. Stock solutions of AuNP–PEG–Chol/FITC (18 nM in DPBS) were diluted to 3 nM in DMEM–HEPES and incubated on cell monolayers 20 min at 37 °C. The solution was removed, and cell monolayers were washed with LCIS. The cell monolayer was imaged in LCIS on confocal laser scanning microscopy (CLSM) using a Nikon A1RSi confocal microscope equipped with a 488 nm argon laser with fluorescence detection channels set to 500–550 nm (green). All images were collected using a Plan Apo 60× objective. Cytotoxicity under the AuNP labeling conditions described above was determined using the CellTiter 96 AQueous One Solution Cell Proliferation Assay (Promega, WI).

DRG Neuron Preparation.

Dorsal root ganglia were removed from 1 to 3 day old Sprague–Dawley rats following euthanasia and were immediately placed in ice-cold DMEM. Ganglia were rinsed multiple times with modified EBSS before digestion with 0.25% trypsin (in EBSS) for 20 min at 37 °C under gentle shaking. The trypsin-digested, softened ganglia were then centrifuged and resuspended in EBSS supplemented with 10% v/v fetal bovine serum (FBS). Next, mechanical trituration with Pasteur pipettes of decreasing tip sizes was performed to yield monodisperse DRG neurons in suspension. Following a final centrifugation, cells were resuspended in DMEM containing 5% v/v FBS. Cells were seeded into sterilized poly-L-lysine solution-treated glass-bottom culture dishes and allowed to sit for 30 min to facilitate DRG neurons adhesion to the glass. A 2.5 mL volume of DMEM added with 5% v/v FBS, 100 U/mL penicillin, and 100 μg/mL streptomycin (supplemented DMEM) was then added to the dish, and the cells were incubated at 37 °C with 5% CO_2 until use.

Experimental Setup for Photoactivation of DRG Neurons.

Dishes containing DRG neurons and bath solution were mounted on a Zeiss IM 35 microscope (Carl Zeiss Microscopy, Thornwood, New York) and visualized through objective lenses ranging from 10× (0.25 NA) to 40× (0.55 NA). Patch pipettes were pulled

on a Sutter Instruments P-2000 CO_2 laser micropipette puller (Novata, California) and flame-polished to produce approximately 2 MΩ resistances when filled with internal pipet solution. An analog waveform from an AD/DA converter board (Innovative Integration SBC-6711-A4D4, Simi Valley, CA) drove the amplifier (Axopatch 200B, Molecular Devices, Sunnyvale, California) to clamp the current through the cell's membrane. The amplifier output, the membrane voltage, was digitized at 16-bit resolution and sampled at 20 kHz by the same AD/DA converter board and stored in a personal computer for analysis. The AD/DA converter board was controlled by customized software. A 532 nm laser system (532 nm DPSS laser, UltraLasers, Ontario, Canada) was mounted and aligned to the central axis of the microscope objective, previously measured power by neutral density filters (Thorlabs Inc., Newton, NJ, United States). TTL-controlled acousto-optic-modulator was used (NEOS Technologies, Gooch & Housego, PLC., Melbourne, Florida) to enable presentation of the faster laser pulses. The focused laser beam, a spot with diameter of about 5 μm (about $\frac{1}{5}$ of the cell diameter), was allowed to move relative to the cell under investigation by an independent manual X–Y micromanipulators system mounted on the microscope. For experiments labeling the inner membrane leaflet with AuNP–PEG–Chol conjugates, the pipet solution was amended with the AuNP conjugates to a final concentration of 1.5 nM. Positive pressure was not applied to the inside of the pipet until contact was made with the target cell.

DRG Neuron Labeling with AuNP–PEG–Chol.

Dishes containing DRG neurons were incubated overnight after the addition of ~260 μL of AuNP-containing preparation (~1.5 nM AuNP in Tyrode's solution containing 5% FBS) or Tyrode's solution alone. On the day of experiment, the supplemented DMEM (containing AuNPs or not) was flushed out and the cells by washing with 10 mL plain Tyrode's solution. A final volume of about 0.5 mL was left in the dish and served as the bathing extracellular solution during the electrophysiological tests to probe photosensitization. Unless otherwise indicated, procedures for the presentation of laser pulses to the cells were similar to those previously described.[4,5] The cytotoxicity of DRG neurons labeled with AuNPs (with and without photoactivation) was determined using the LIVE/DEAD Viability kit (ThermoFisher).

Supplementary Material

Refer to Web version on PubMed Central for supplementary material.

Acknowledgments

Funding

The authors acknowledge the support of the NRL Institute for Nanoscience and Base Funding Program (Work Units MA04106–41-T008–15 and MA041–06-41–4943) and NIH grants R01-GM030376, R21-EY023430, and R21-EY027101.

REFERENCES

(1). Bucharskaya A, Maslyakova G, Terentyuk G, Yakunin A, Avetisyan Y, Bibikova O, Tuchina E, Khlebtsov B, Khlebtsov N, and Tuchin V (2016) Towards Effective Photothermal/Photo-dynamic Treatment Using Plasmonic Gold Nanoparticles. Int. J. Mol. Sci. 17, 1295.

(2). Rosa S, Connolly C, Schettino G, Butterworth KT, and Prise KM (2017) Biological Mechanisms of Gold Nanoparticle Radiosensitization. Cancer Nanotechnol. 8, 2. [PubMed: 28217176]

(3). Schuemann J, Berbeco R, Chithrani DB, Cho SH, Kumar R, McMahon SJ, Sridhar S, and Krishnan S (2016) Roadmap to Clinical Use of Gold Nanoparticles for Radiation Sensitization. Int. J. Radiat. Oncol., Biol., Phys. 94, 189–205. [PubMed: 26700713]

(4). Carvalho-de-Souza JL, Treger JS, Dang B, Kent SBH, Pepperberg DR, and Bezanilla F (2015) Photosensitivity of Neurons Enabled by Cell-Targeted Gold Nanoparticles. Neuron 86, 207–217. [PubMed: 25772189]

(5). Carvalho-de-Souza JL, Pinto BI, Pepperberg DR, and Bezanilla F (2018) Optocapacitive Generation of Action Potentials by Microsecond Laser Pulses of Nanojoule Energy. Biophys. J. 114, 283–288. [PubMed: 29273263]

(6). Shapiro MG, Homma K, Villarreal S, Richter C-P, and Bezanilla F (2012) Infrared Light Excites Cells by Changing Their Electrical Capacitance. Nat. Commun. 3, 736. [PubMed: 22415827]

(7). Kubota T, Dang B, Carvalho-de-Souza JL, Correa AM, and Bezanilla F (2017) Nav Channel Binder Containing a Specific Conjugation-Site Based on a Low Toxicity β-scorpion Toxin. Sci. Rep. 7, 16329. [PubMed: 29180755]

(8). Engberg O, Hautala V, Yasuda T, Dehio H, Murata M, Slotte JP, and Nyholm TKM (2016) The Affinity of Cholesterol for Different Phospholipids Affects Lateral Segregation in Bilayers. Biophys. J. 111, 546–556. [PubMed: 27508438]

(9). Silvius JR (2003) Role of Cholesterol in Lipid Raft Formation: lessons from lipid model systems. Biochim. Biophys. Ada, Biomembr. 1610, 174–183.

(10). Nag OK, Naciri J, Oh E, Spillmann CM, and Delehanty JB (2016) Lipid Raft-Mediated Membrane Tethering and Delivery of Hydrophobic Cargos from Liquid Crystal-Based Nanocarriers. Bioconjugate Chem. 27, 982–993.

(11). Nag OK, Naciri J, Erickson JS, Oh E, and Delehanty JB (2018) Hybrid Liquid Crystal Nanocarriers for Enhanced Zinc Phthalocyanine-Mediated Photodynamic Therapy. Bioconjugate Chem. 29, 2701–2714.

(12). Yu X, Wang J, Feizpour A, and Reinhard BM (2013) Illuminating the Lateral Organization of Cell-Surface CD24 and CD44 through Plasmon Coupling between Au Nanoparticle Immunolabels. Anal. Chem. 85, 1290–1294. [PubMed: 23320416]

(13). Oh E, Susumu K, Goswami R, and Mattoussi H (2010) One-Phase Synthesis of Water-Soluble Gold Nanoparticles with Control over Size and Surface Functionalities. Langmuir 26, 7604–7613. [PubMed: 20121172]

(14). Oh E, Delehanty JB, Sapsford KE, Susumu K, Goswami R, Blanco-Canosa JB, Dawson PE, Granek J, Shoff M, Zhang Q, et al. (2011) Cellular Uptake and Fate of PEGylated Gold Nanoparticles Is Dependent on Both Cell-Penetration Peptides and Particle Size. ACS Nano 5, 6434–6448. [PubMed: 21774456]

(15). Oh E, Fatemi FK, Currie M, Delehanty JB, Pons T, Fragola A, Lévêque-Fort S, Goswami R, Susumu K, Huston AL, and Medintz IL (2013) PEGylated Luminescent Gold Nano-clusters: Synthesis, Characterization, Bioconjugation, and Application to One- and Two-Photon Cellular Imaging. Part. Part. Syst. Char. 30, 453–466.

(16). Jiang Y, Carvalho-de-Souza JL, Wong RCS, Luo Z, Isheim D, Zuo X, Nicholls AW, Jung IW, Yue J, Liu D-J, et al. (2016) Heterogeneous Silicon Mesostructures for Lipid-Supported Bioelectric Interfaces. Nat. Mater. 15, 1023. [PubMed: 27348576]

(17). Rost BR, Schneider-Warme F, Schmitz D, and Hegemann P (2017) Optogenetic Tools for Subcellular Applications in Neuroscience. Neuron 96, 572–603. [PubMed: 29096074]

(18). Martino N, Feyen P, Porro M, Bossio C, Zucchetti E, Ghezzi D, Benfenati F, Lanzani G, and Antognazza MR (2015) Photothermal Cellular Stimulation in Functional Bio-Polymer Interfaces. Sci. Rep. 5, 8911. [PubMed: 25753132]

(19). Fabbro A, Sucapane A, Toma FM, Calura E, Rizzetto L, Carrieri C, Roncaglia P, Martinelli V, Scaini D, Masten L, et al. (2013) Adhesion to Carbon Nanotube Conductive Scaffolds Forces Action-Potential Appearance in Immature Rat Spinal Neurons. PLoS One 8, No. e73621.

(20). Sytnyk M, Jakešová M, Litviňuková M, Mashkov O, Kriegner D, Stangl J, Nebesářová J, Fecher FW, Schöfberger W, Sariciftci NS, et al. (2017) Cellular interfaces with hydrogen-bonded organic semiconductor hierarchical nanocrystals. Nat. Commun. 8, 91. [PubMed: 28733618]

(21). Govorov AO, and Richardson HH (2007) Generating Heat with Metal Nanoparticles. Nano Today 2, 30–38.

(22). Jain PK, Lee KS, El-Sayed IH, and El-Sayed MA (2006) Calculated Absorption and Scattering Properties of Gold Nanoparticles of Different Size, Shape, and Composition: Applications in Biological Imaging and Biomedicine. J. Phys. Chem. B 110, 7238–7248.

(23). Boeneman K, Delehanty JB, Blanco-Canosa JB, Susumu K, Stewart MH, Oh E, Huston AL, Dawson G, Ingale S, Walters R, Domowicz M, et al. (2013) Selecting Improved Peptidyl Motifs for Cytosolic Delivery of Disparate Protein and Nanoparticle Materials. ACS Nano 7, 3778–3796. [PubMed: 23710591]

(24). Baffou G, Quidant R, and García de Abajo FJ (2010) Nanoscale Control of Optical Heating in Complex Plasmonic Systems. ACS Nano 4, 709–716. [PubMed: 20055439]

(25). Chan CH (1975) Effective Absorption for Thermal Blooming Due to Aerosols. Appl. Phys. Lett. 26, 628–630.

(26). Govorov AO, Zhang W, Skeini T, Richardson H, Lee J, and Kotov NA (2006) Gold Nanoparticle Ensembles as Heaters and Actuators: Melting and Collective Plasmon Resonances. Nano-scale Res. Lett. 1, 84.

(27). Radwan AA, and Alanazi FK (2014) Targeting Cancer Using Cholesterol Conjugates. Saudi Pharm. J. 22, 3–16. [PubMed: 24493968]

(28). Steichen SD, Caldorera-Moore M, and Peppas NA (2013) A Review of Current Nanoparticle and Targeting Moieties for The Delivery of Cancer Therapeutics. Eur. J. Pharm. Sci. 48, 416–427. [PubMed: 23262059]

(29). Lee H, Venable RM, MacKerell AD, and Pastor RW (2008) Molecular Dynamics Studies of Polyethylene Oxide and Polyethylene Glycol: Hydrodynamic Radius and Shape Anisotropy. Biophys. J. 95, 1590–1599. [PubMed: 18456821]

(30). Daniel M, Řezníčková J, Handl M, Iglič A, and Kralj-Iglič V (2018) Clustering and Separation of Hydrophobic Nanoparticles in Lipid Bilayer Explained by Membrane Mechanics. Sci. Rep. 8, 10810. [PubMed: 30018296]

(31). Paramelle D, Nieves D, Brun B, Kraut RS, and Fernig DG (2015) Targeting Cell Membrane Lipid Rafts by Stoichiometric Functionalization of Gold Nanoparticles with a Sphingolipid-Binding Domain Peptide. Adv. Healthcare Mater. 4, 911–917.

(32). Valenza M, Chen JY, Di Paolo E, Ruozi B, Belletti D, Ferrari Bardile C, Leoni V, Caccia C, Brilli E, Di Donato S, et al. (2015) Cholesterol-Loaded Nanoparticles Ameliorate Synaptic and Cognitive Function in Huntington's Disease Mice. EMBO Mol. Med. 7, 1547–1564. [PubMed: 26589247]

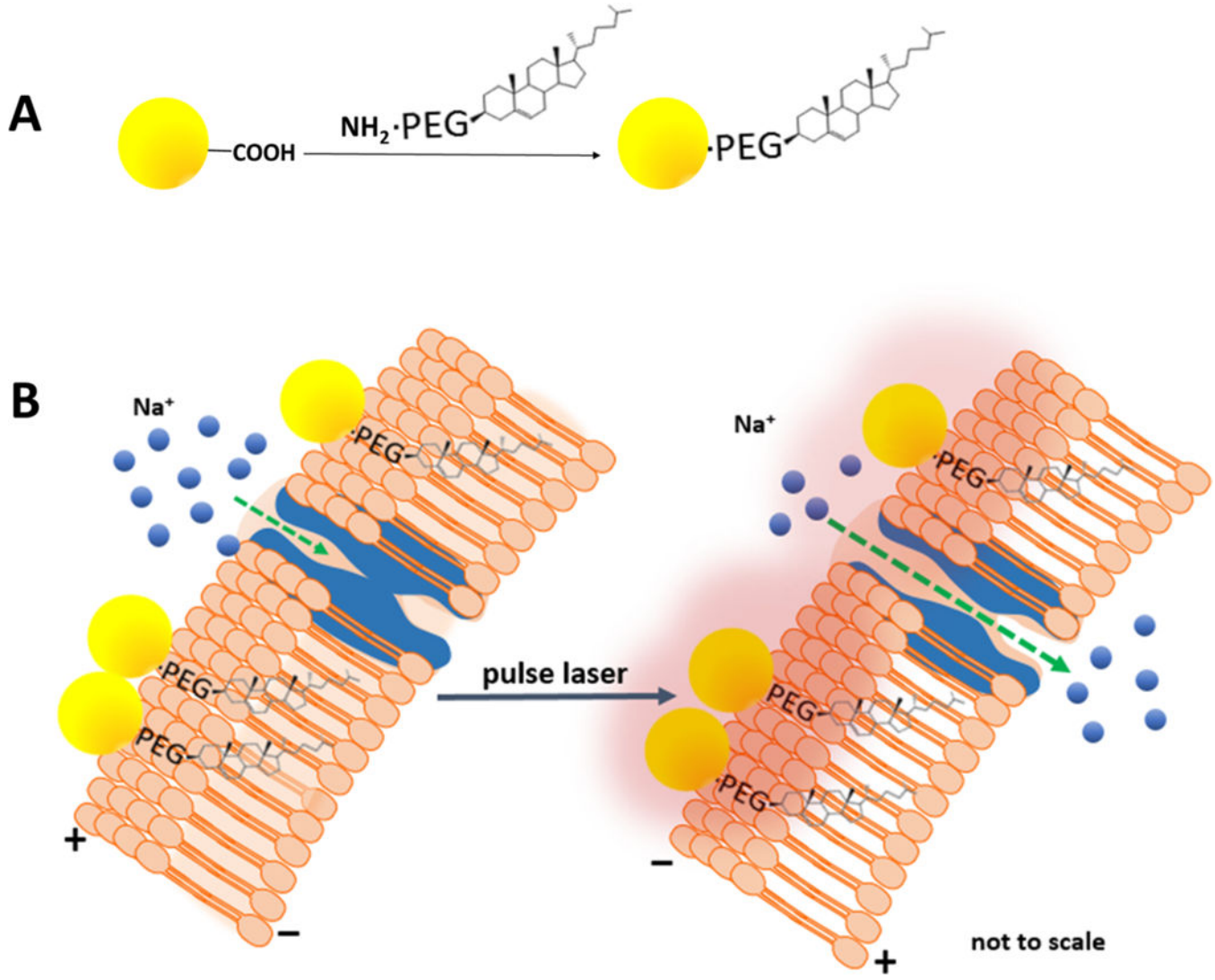

Figure 1.

Structure and operation of the AuNP–PEG–Chol conjugate. (A) Functionalization of the 20 nm spherical AuNP (yellow sphere) with PEG–Chol using EDC chemistry which forms an amide bond between the TA–PEG–COOH and the PEG–Chol (see Experimental Methods). (B) Proposed interfacing of AuNP–PEG–Chol with the cell plasma membrane and light-induced activity. Plasmonic light absorption by the AuNP in response to a laser pulse induces, via a plasma membrane temperature increase, a capacitive current that results in opening of membrane-resident Na_Vs (blue transmembrane structures), the inward passage of sodium ions (blue spheres), and resulting AP generation. In both panels, illustrated structures are not shown to scale.

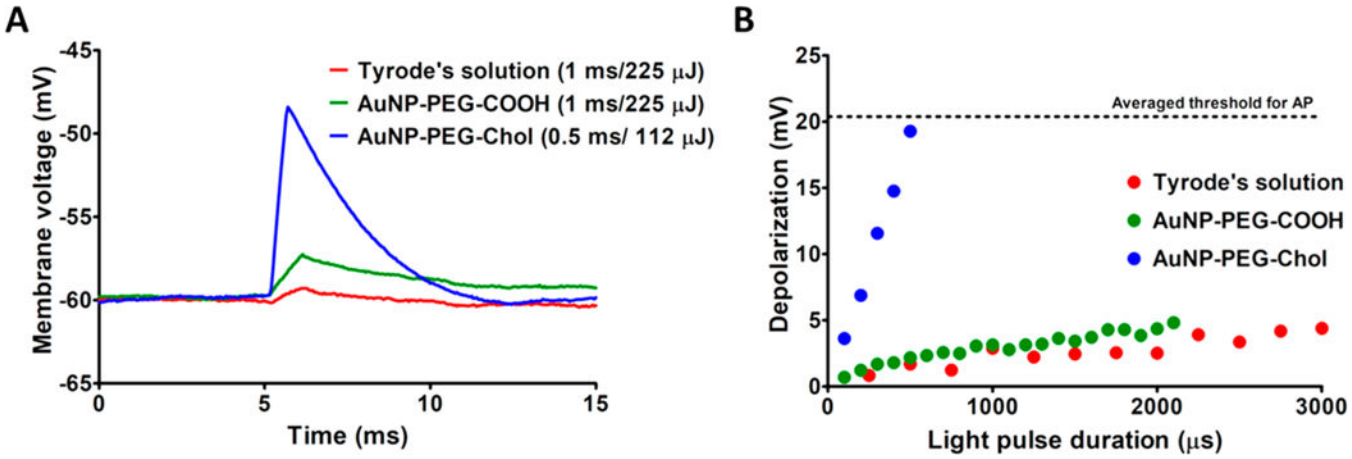

Figure 2.

Subthreshold photosensitivity of DRG neurons. (A) Preparations of DRG neurons were incubated overnight in growth medium amended with either AuNP–PEG–Chol, AuNP-PEG-COOH, or Tyrode's solution. Before use, all dishes were flushed with Tyrode's solution to remove nonspecifically bound AuNPs. The data show the current-clamp ($I = 0$) response of a single neuron from each preparation following treatment with AuNP–PEG–Chol (blue), AuNP-PEG-COOH (green), or Tyrode's solution only (red). (B) Subthreshold membrane depolarizations exhibited in response to a 225 mW laser pulse of varying duration. The illustrated results are from the same three DRG neurons as those described in A. The dashed line represents the average threshold depolarization for AP generation, based on data obtained from the three DRG neurons described in A and from an additional 15 cells (data not shown).

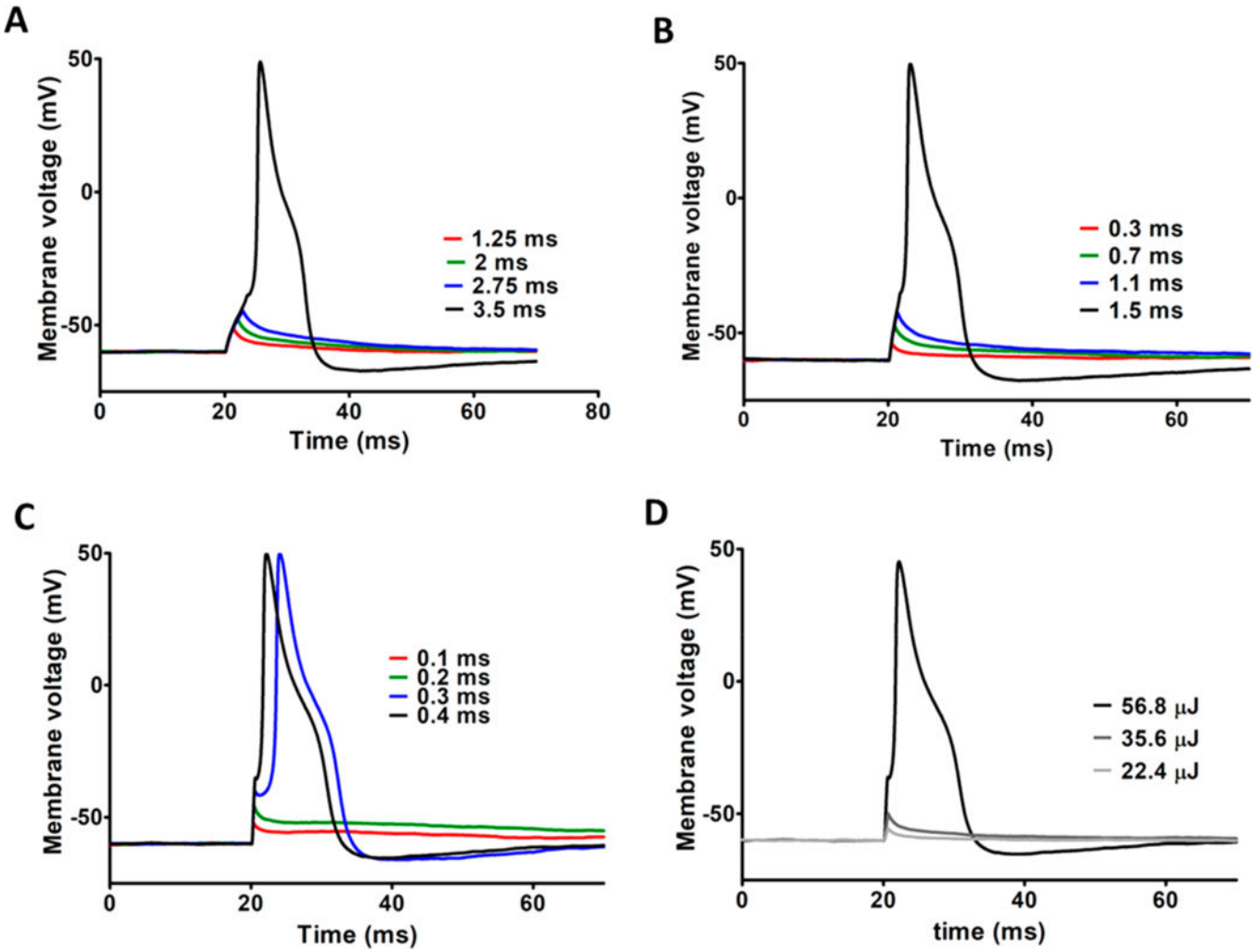

Figure 3.

AP generation in AuNP–PEG–Chol treated neurons as a function of laser pulse power and duration. Shown are results obtained with light pulses of 45 mW power and durations of 1.25–3.5 ms (A), 71 mW power and durations of 0.3–1.5 ms (B), 142 mW power and durations of 0.1–0.4 ms (C), and fixed-duration flashes (0.4 ms) and total energies 22.4–56.8 μJ (D).

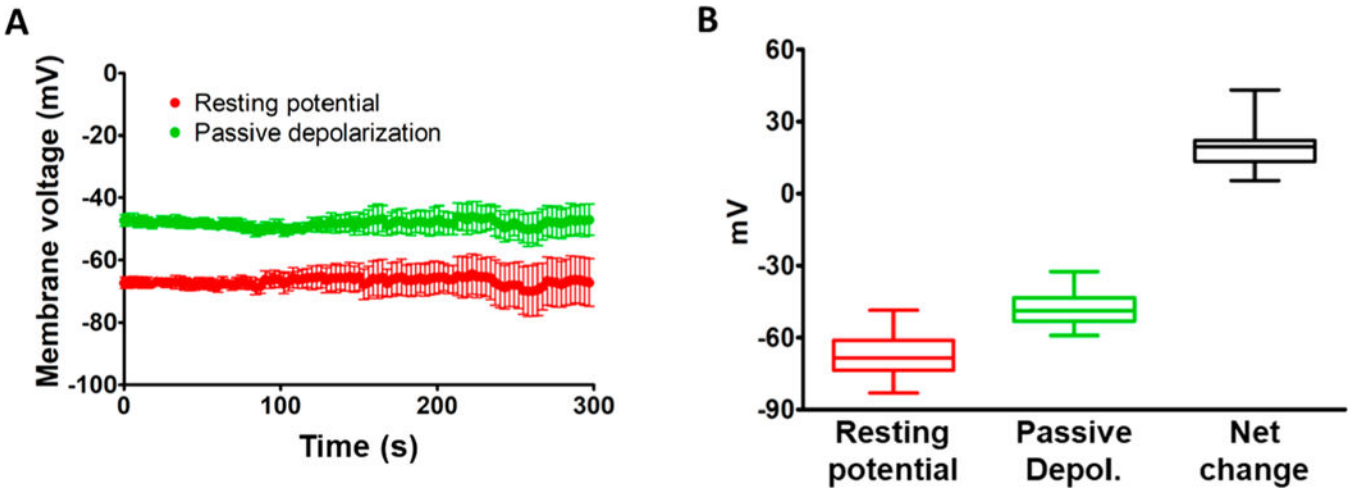

Figure 4.

Time-dependence of passive depolarization mediated by AuNP–PEG–Chol. (A) Red symbols, resting potentials (mean ± SEMs) of 4–15 cells determined over a 5 min period. Green symbols, passive depolarizations (mean ± SEMs) directly induced by the laser pulse. The number of cells described by the data decreased from an initial population of 15 down to 4 during the period of investigation (due to loss of the patch seal on a number of cells), and the progressive increase in SEMs determined over this period can be attributed to this decreasing population. (B) Summary of the data presented in panel A. Red, green, and black symbols indicate data obtained for resting potential, potential at the peak of passive laser-induced depolarization, and the net change induced by this depolarization, respectively. See text for further details.

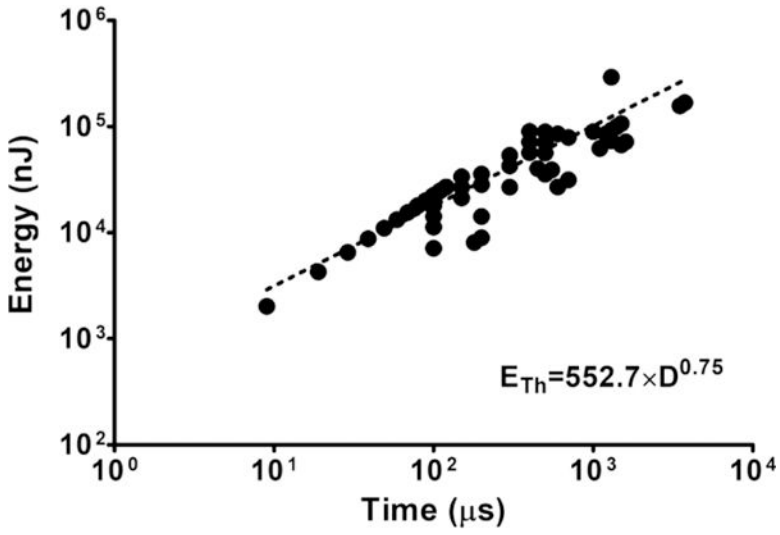

Figure 5.

Flash energy at action potential threshold for AuNP–PEG–Chol-labeled DRG neurons as a function of time (flash duration). Data points represent determinations of minimal flash energy needed for action potential generation (threshold) at a given flash duration. The data show results obtained from a total of 6 cells (minimum of 20 data points collected per cell). The dashed line fitted to the data plots the power function equation $E_{Th} = a \times D^b$ (lower right). The values of a and b were determined to be 552.7 nJ and 0.75, respectively. See main text for detailed description.

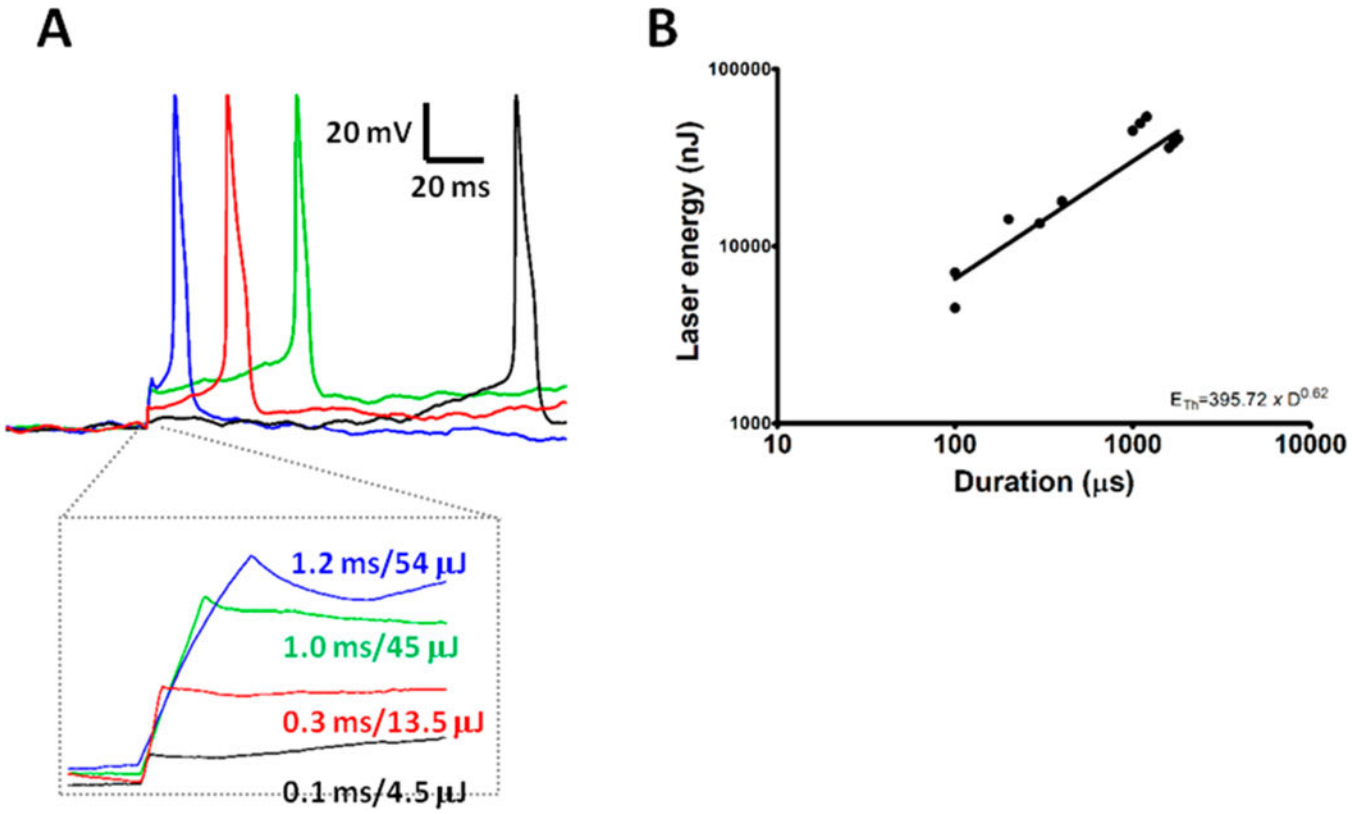

Figure 6.

Intracellular delivery of AuNP–PEG–Chol mediates action potential generation. (A) Action potentials triggered by laser pulses of fixed power and varying duration exhibited by a single DRG cell labeled with AuNP–PEG–Chol on the inner leaflet of the plasma membrane. (B) Laser pulse energy E_{th} at action potential generation threshold as a function of pulse duration, plotted in log–log format, for the cell described in panel A. The line fitted to the data plots the power function equation as described in Figure 5. Values of *a* and *b* correspond to 395.72 nJ and 0.62, respectively.